Cement and Concrete Research 39 (2009) 1230–1238

Contents lists available at ScienceDirect

Cement and Concrete Research

journal homepage: http://ees.elsevier.com/CEMCON/default.asp

Self-consolidating concrete subjected to high temperature Mechanical and physicochemical properties

Hanaa Fares *, Albert Noumowe, Sébastien Remond

L2MGC Université de Cergy-Pontoise, F-95000 Cergy-Pontoise, France

ARTICLE INFO

Article history:
Received 27 November 2008
Accepted 3 August 2009

Keywords:
Self-consolidating concrete
Temperature (A)
Mechanical properties (C)
Physical properties (C)
Permeability (C)

ABSTRACT

This paper presents an experimental study on the performance of self-consolidating concrete (SCC) subjected to high temperature. Two SCC mixtures and one vibrated concrete were tested. These concrete mixes were developed in the French National Project B@P. Mechanical and microstructural properties were studied at ambient temperature and after heating. We studied compressive strength, flexural strength, bulk modulus of elasticity, porosity and permeability. For each test, the specimens were heated at a rate of 1 °C/min up to different temperatures (150, 300, 450 and 600 °C). In order to ensure a uniform temperature throughout the specimen, the temperature was held constant at the target temperature for 1 h before cooling. In addition, the specimen mass was measured before and after heating in order to determine the loss of water during the test. The results allowed us to analyze the degradation of SCC and vibrated concretes due to heating.

1. Introduction

The use of self-consolidating concrete (SCC) was considerably developed during the last years and a growing attention is brought to the study of its mechanical properties at hardened state. The characteristics of this concrete (large paste volume, high content of mineral admixtures, coarse to fine aggregates ratio close to 1,) linked to its placing conditions could modify its mechanical behaviour, comparatively to traditional vibrated concrete. The behaviour of SCC subjected to high temperature has in particular to be evaluated.

In case of fire, concrete is exposed to high temperature that induces a material degradation: strength decrease, cracking, and in certain conditions spalling can occur. Up to now, the effect of elevated temperature has been studied essentially on vibrated and on high performance concretes. But, what about the behaviour of SCC at high temperature? The few studies on SCC subjected to high temperature show both a decrease in strength and an increase in the risk of spalling [1–3] or a behaviour similar to that of vibrated concrete [4–6].

The aim of this study is to analyze the mechanical behaviour of SCC subjected to high temperature. Three mixes were investigated: two SCC and one vibrated concrete (VC). The mechanical strengths at 90 days were 37, 54 and 41 MPa for SCC 1, SCC 2 and VC (respectively).

2. Materials

2.1. Cement

Table 1 presents the mineralogical composition and the main physical characteristics of the cements used. We used a CEM I for SCC 2 and VC and a CEM II/B for the SCC 1.

2.2. Aggregates

Crushed coarse aggregate (4/22.5) and quarry sand (0/4) were used. Their physical and chemical characteristics are presented in Table 2.

2.3. Limestone fillers

Limestone fillers BETOCARB P2-MX, complying with French standard NF P 18-508 [7] were used. Their physical and chemical characteristics are presented in Table 3.

2.4. Admixtures

A superplasticizer CIMFLUID 2002 based on a modified polycarboxylate was employed to obtain a satisfactory fluidity for the different mixes. Its density at 20 °C is 1100 kg m^{-3}, its pH is 7, and the dried content is 34.76%.

A viscosity-enhancing admixture COLLAXIM RT was also used to improve the concrete stability of the two SCC. This product is complying with standard EN 206-1 [8]. Its density at 20 °C is 970 kg m^{-3}, its pH is

* Corresponding author.
E-mail address: hanaafares@yahoo.fr (H. Fares).

0008-8846/$ – see front matter © 2009 Elsevier Ltd. All rights reserved.
doi:10.1016/j.cemconres.2009.08.001

Table 1
Mineralogical composition and main physical characteristics of the cements.

Cement	CEM I 52.5 N CE CP2 NF	CEM II/B-(LL-S) 32.5 R CE CP2 NF
Origin	Villier au Bouin	Gaurain
Bogue composition		
C_3S (%)	66.9	70.23
C_2S (%)	10.7	7.66
C_3A (%)	8.4	8.43
C_4AF (%)	7.6	7.22
Physical properties		
Absolute density	3.13	3.04
Blaine surface ($m^2\ g^{-1}$)	359	348.3
Strength Rc_{28} (MPa)	61.3	47.8

7.8, and the dried content is 1.77. The advised content is 0.05–0.5 kg for 100 kg of cement.

2.5. Mixture proportions

The three concrete mixes investigated in our research were developed in the French National Project B@P. Table 4 presents their mixture proportions. The concrete mixes contain the same constituents (except the cement that was adapted to the target strength), a similar granular skeleton and a water/powder ratio equal to 0.36, 0.42 and 0.54 (powder: C + A). The admixture content was determined so as to obtain a slump flow larger than 65 cm for SCC [9–11].

Each concrete mixture was cast in cylindrical molds of 16 cm in diameter and 32 cm in height and 15 cm in diameter and 30 cm in height, and in prismatic molds with dimensions 10 cm × 10 cm × 40 cm. After curing for 90 days in sealed plastic bags, the concrete specimens were subjected to the different heating cycles. The curing conditions referred to RILEM recommendations [12], which advocate a preserving of at least 90 days before testing.

3. Tests

3.1. Test temperature

The specimens were subjected to four different temperature cycles up to 150, 300, 450 and 600 °C. The first part of each cycle consisted of a heating at 1 °C/min up to the target temperature. After that, the temperature was held constant for 1 h in order to ensure uniform temperature throughout the specimens. The last part of the cycles consisted of a cooling down to ambient temperature. The rate of heating refers to the recommendations of the RILEM Technical Committee TC-129 [12].

Fig. 1 presents the theoretical evolutions of temperature as a function of time for the four temperature cycles. The real evolution of temperature obtained with a heating up to 300 °C is also indicated. We observe that the real temperature is very close to the theoretical evolution during heating, whereas the cooling is slower which reduces the risk of thermal shock.

Table 2
Physical and chemical characteristics of the aggregates.

Aggregates	0/4	4/22.5
Chemical analysis		
SiO_2 (%)	75	70
$CaCO_3$ (%)	20	25
Feldspaths (%)	4	5
Others minerals (%)	Traces	Traces
Physical properties		
Absolute density	2.6	2.5

Table 3
Physical and chemical characteristics of the limestone fillers.

Fillers	BETOCARB P2 — MX
Origin	Maxey sur Vaise
Chemical analysis	
$CaCO_3$ (%)	98.4
SiO_2 (%)	0.2
Na_2O (%)	0.009
Soufre (%)	0.041
Physical properties	
Absolute density	2.6
Apparent density	0.6
Blaine surface ($m^2\ g^{-1}$)	755
Activity index i_{28}	0.80
Proportion smaller than 63 μm (%)	96.1
Proportion smaller than 125 μm (%)	99.9
Proportion smaller than 2 mm (%)	100

3.2. Specimens in the oven

For each mix and each temperature cycle, eleven specimens were stored in the oven. Each batch was composed of four cylindrical specimens Ø 16 × 32 cm, four cylindrical specimens Ø 15 × 5 cm (which were cut in the cylinders Ø 15 × 30 cm) for the permeability tests and three prismatic specimens 10 × 10 × 40 cm.

All the specimens were stored in the oven in the same condition in order to have a uniform temperature. Fig. 2 shows the layout of the oven with the specimens.

3.3. Mechanical tests

3.3.1. Compressive strength and bulk modulus of elasticity

The compressive strength was first determined according to standard NF EN 12390-3 [13] with one cylindrical specimen Ø 16 × 32 cm. Then, the bulk modulus of elasticity was measured with the three other cylindrical specimens Ø 16 × 32 cm. Three loading–unloading cycles (0.5 MPa/s) between 0.5 MPa and the third of the compressive strength obtained with the preliminary test were performed. After three cycles, the specimen was loaded and the compressive strength was determined. The bulk modulus of elasticity corresponds to the mean value of secant modulus obtained with the two last cycles [14]. The compressive strength is the mean value of four values of compressive strength with the four cylindrical specimens Ø 16 × 32 cm.

3.3.2. Flexural strength

NF EN 12390-5 [15] was followed to characterize the flexural strength of concrete. This test was realized on three prismatic specimens for each mix and each temperature.

Table 4
Mixture proportions.

1 m^3	SCC 1	SCC 2	VC
CEM I 52.5 N	–	350	373
CEM II 32.5 R	328	–	–
Limestone filler	225	130	–
Sand 0/4	795	857	913
Coarse aggregates 4/22.5	745	742	790
Water	199	200	202
Slump test or flow (cm)	65	71	19
Paste volume (liters)	393.4	361.8	321.2
Water/cement	0.61	0.57	0.54
Water/powder	0.36	0.42	0.54
Filler/powder	0.41	0.27	0
Coarse agg./Fine agg.	0.94	0.87	0.87
Mwater/Mconcrete (%)	8.86	8.78	8.87
Strength at 90 days (MPa)	37	54	41

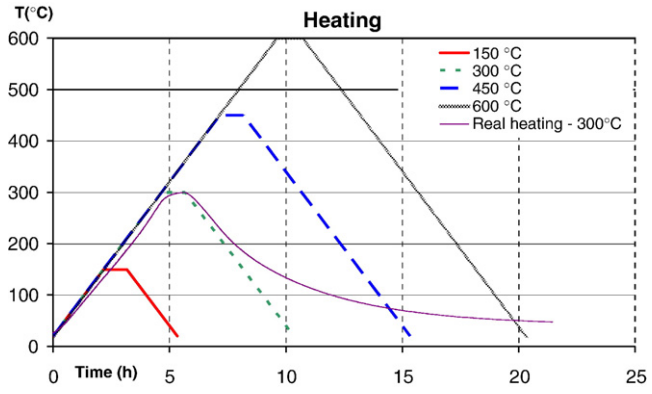

Fig. 1. Heating and cooling curves.

3.4. Physical and chemical properties

3.4.1. Concrete mass loss

The mass of each specimen was measured before and after each temperature cycle. This allows us to quantify the dehydration of concrete after each heating.

3.4.2. Porosity and density

Density and total porosity of the different mixes were studied. These properties were measured before and after each temperature cycle. The testing conditions were similar to those recommended by AFPC-AFREM [16]. Three samples were tested for each concrete and each temperature cycle. The porosity corresponds to the mean value obtained.

Before testing, samples were kept in plastic bags, then they were weighted and put in an oven at 75 °C until constant mass. Samples were then immersed into water and weighted regularly until they were completely saturated. The immersed mass was determined with a hydrostatic balance, then the samples were wiped in order to remove the surface excess water, and the saturated mass was measured. Considering the brittleness of the heated samples at 600 °C, the results corresponding to this temperature are less accurate.

The porosity is determined according to Eq. (1):

$$\varepsilon = \frac{M_{sat} - M_{dry}}{V} = \frac{M_{sat} - M_{dry}}{M_{sat} - M_{sat}^{imm}} \quad (1)$$

where, M_{sat} and M_{sat}^{imm} are the saturated mass of a sample measured in the air and in water respectively. M_{dry} is the mass of dried specimen, weighted in air. The apparent density ρ_d of the specimen for each mix and each temperature is also determined (Eq. (2)).

$$\rho_d = \frac{M_{dry}}{V} = \frac{M_{dry}}{M_{sat} - M_{sat}^{imm}}. \quad (2)$$

3.4.3. Permeability

To measure the permeability, cylindrical specimens Æ 15×5 cm were cut in cylinders Æ 15×30 cm. Only the central part of the cylinders (a, b, c and d in Fig. 3) was kept for the measures.

The residual permeability obtained after each temperature cycle was determined and compared to that obtained with dried specimens stored at 75 °C until constant mass [16,17]. After drying, specimens were stored in plastic bags during 24 h before testing. Heated specimens were tested 24 h ± 4 h after cooling in order to maintain the same hydric conditions for all the specimens.

A CEMBUREAU permeameter was used to measure permeability [18]. This test gives the apparent permeability k_a of the material depending on the injection pressure. To determine the intrinsic permeability k_v, we use the correction proposed by Klinkenberg [19], (Eq. (3)). The value of b^* is a function of the porosity, nature of the used gas and is obtained by linear interpolation.

$$k_a = k_v\left(1 + \frac{b^*}{\overline{P}}\right) \quad (3)$$

with:

k_a: apparent permeability (m^2)
k_v: intrinsic permeability (m^2)
b^*: Klinkenberg coefficient
P: average pressure (Pa).

4. Results and discussion

4.1. Initial mechanical strength

The mechanical properties (compressive strength, flexural strength and modulus of elasticity) and slump flow of the tested concretes before heating are presented in Table 5 and compared with the values obtained in the French National Project B@P with the same concrete mixes.

We observe in Table 5 that the dispersions obtained for the compressive strength and for the modulus of elasticity of the two SCCs are much lower than for the vibrated concrete. This is due to the higher homogeneity and reproducibility of SCC in comparison to vibrated concrete. The dispersion obtained for the vibrated concrete is quite large. However, despite the dispersion, the mean values obtained in our study for all the concretes are very close to those of the French National Project. In the rest of the paper, all the mechanical properties studied are relative residual properties, compared to the average initial properties presented in Table 5.

4.2. Thermal stability

During our tests, spalling has been observed for SCC 1 and SCC 2 during the heating up to 450 °C and 600 °C. Spalling occurred around

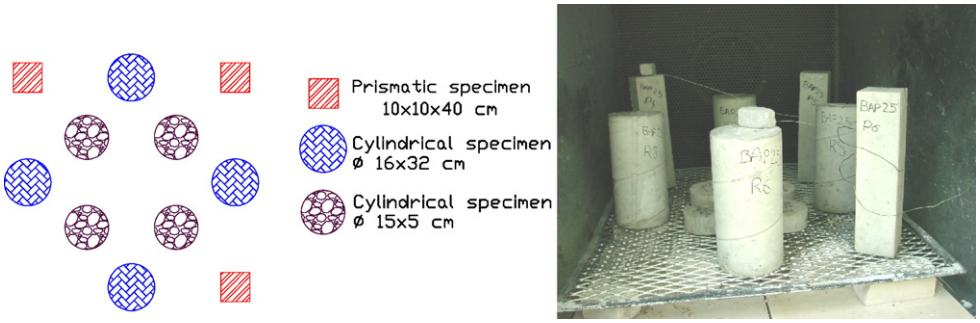

Fig. 2. Layout of the specimens in the oven.

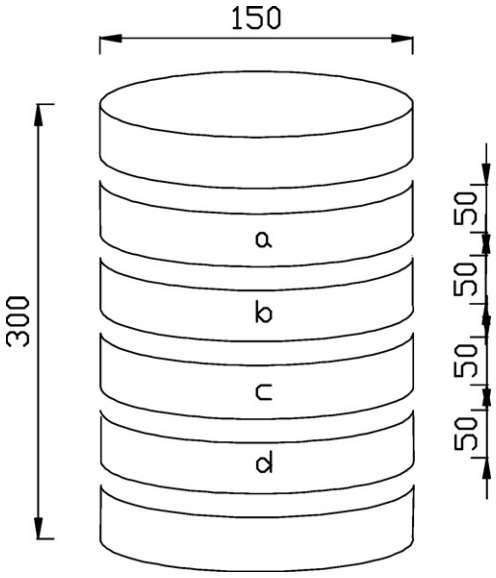

Fig. 3. Preparation of specimens for permeability tests.

315 °C and concerned only the cylindrical specimens Ø 16×32 cm (Fig. 4). This observation agrees with Kanema's results [20].

The two SCC which spalled (SCC 1 and SCC 2) possessed an initial compressive strength equal to 37 and 54 MPa respectively. Comparatively, the specimens which did not spall after heating (VC) have a compressive strength equal to 41 MPa. Spalling has therefore been observed for SCC presenting a moderate compressive strength, whereas it is generally observed for high performance concrete with vibrated concretes. Some authors [21–25] have already observed that the risk of spalling is more pronounced for SCC than for vibrated concrete. Our study confirms these results.

Because of spalling, the residual compressive strength of SCC 1 and SCC 2 at 450 and 600 °C have only been determined with at least 2 specimens (at 450 °C with 2 specimens, at 600 °C with 3 specimens).

4.3. Mechanical strength after thermal treatment

4.3.1. Residual compressive strength

Residual properties (measured after heating and cooling) were compared to initial properties.

Fig. 5 presents the variation of the residual compressive strength versus the temperature (the error bars represent the standard deviation obtained for each concrete at each temperature cycle). Our results are compared with the values proposed by the Eurocode 4.1.2 — Annex C [26]. These values show the evolution of relative residual compressive strength with temperature on vibrated concretes.

The behaviour of SCC and vibrated concrete differs significantly between 20 and 300 °C. On one hand, for the two SCC, after a moderate decrease in compressive strength between 20° and 150 °C, an important increase (about 25%) is observed between 150 and 300 °C. On the other hand, for the vibrated concrete (VC), the relative compressive strength decreases monotonically. However, the decrease observed between 150 and 300 °C for VC is moderate (about 5%), and given the large standard deviation observed for this concrete, this result cannot be generalized. Beyond 300 °C, an important decrease in strength is observed for all the mixes.

Table 5
Initial mechanical properties and comparison with French National Project [9].

(MPa)	SCC 1			SCC 2			VC		
Tested concretes									
Slump (cm)	65			71			19		
Compressive strength	34.6	36.7	38.6	55.5	51	54.6	46.9	35.8	39.7
Average compressive strength	36.6			53.7			40.8		
Standard deviation of σ_c	2.0			2.4			5.7		
Flexural strength	4.5	4.7	4.0	5.2	6.3	6.3	5.1	4.8	4.2
Average flexural strength	4.4			5.9			4.7		
Standard deviation of σ_{fl}	0.4			0.6			0.4		
Modulus of elasticity	35,420	36,160	36,722	38,725	39,864	38,429	40,105	44,000	47,700
Average modulus of elasticity	36,111			38,429			43,935		
Standard deviation of E	655			758			3798		
French National Project about SCC									
Compressive strength	37.4			56			42		
Slump (cm)	68			68			–		

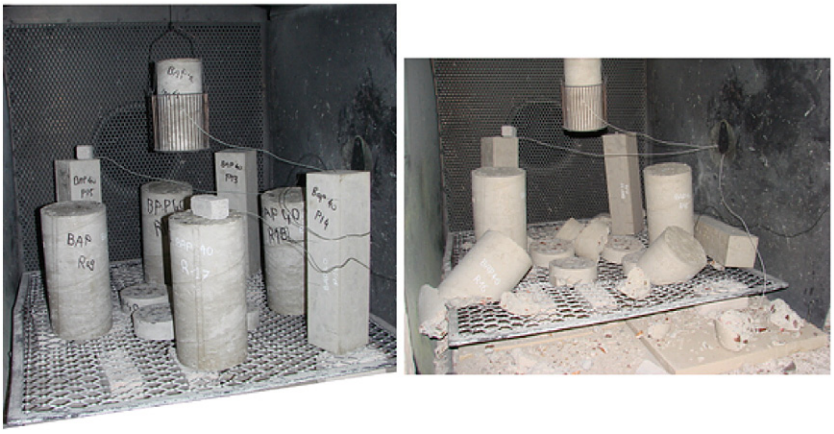

Fig. 4. Specimens before and after thermal treatment.

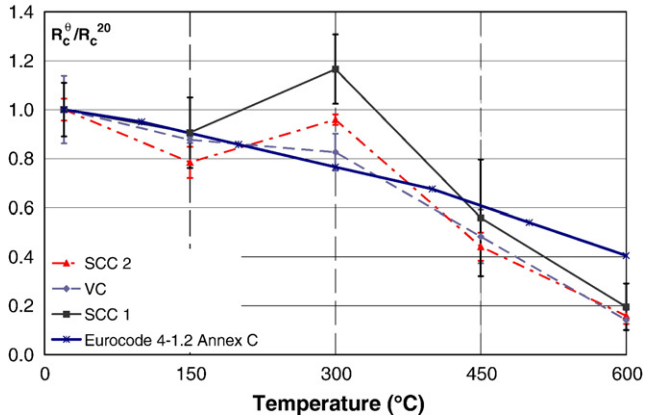

Fig. 5. Relative residual compressive strength.

All the relative residual compressive strengths measured are similar to the values determined according to standards [26], except at 300 °C for the SCC.

The decrease in strength between 20 and 150 °C has already been observed on vibrated concretes [20,27–29]. According to Khoury [29], this decrease corresponds to a reduction of the cohesion of Van der Waal forces between the C–S–H layers. This reduces the surface energy of C–S–H and leads to the formation of silanol groups (Si–OH: OH–Si) that presents weaker bonding strength.

The other point is the increase in strength between 150 and 300 °C. Several hypotheses have been proposed in the literature to explain this increase. Dias et al. [26] attribute it to a rehydration of the paste due to the migration of water in the pores. In another study, Khoury [29] assumes that the silanol groups lose a part of their bonds with water, which induces the creation of shorter and stronger siloxane elements (Si–O–Si) with probably larger surface energies that contribute to the increase in strength. This increase in strength was also observed by Xu who carried out microhardness tests on hardened cement paste and interfacial transition zone [30].

However the previous hypotheses do not allow explaining the difference between SCC and the vibrated concrete. Nevertheless, this difference of behaviour is small in comparison to the dispersion of results concerning the VC and it is not observed systematically in the literature [4–6]. Moreover, the increase in compressive strength between 150 and 300 °C has already been observed on vibrated concretes [20,27,31–33].

4.3.2. Residual flexural strength

Fig. 6 presents the variation of the residual flexural strength as a function of the temperature. The residual flexural strength of SCC decreases continuously while we observe stabilization or a small increase for VC between 150 and 300 °C. Beyond 300 °C, the strength decreases very quickly for all the mixes. However, given the dispersion of the results, we can conclude that the evolution of residual flexural strength with temperature is the same for all the studied concretes.

These results agree with that of Xu [30] who showed with microhardness test on ordinary concrete that the interfacial transition zone is affected by the heating: the ITZ is weakened by the appearance of cracks.

The loss of indirect tensile strength for SCC and VC subjected to high temperatures was clearly different from the more gradual loss of compressive strength. This is because many micro and macro cracks were produced in the specimens due to the thermal incompatibility between aggregates and cement paste [29,34]. The cracking degree influences more importantly the flexural strength than the compressive strength [34,35]. The cracks generated by a heating up to 300 °C do not lead therefore to a reduction of compressive strength [30], but lead to a reduction of tensile strength, and so of flexural strength as well.

4.3.3. Residual bulk modulus of elasticity

Fig. 7 presents the stress–strain curves obtained for SCC 2 with the temperature.

Fig. 7 shows the stress–strain curves obtained for SCC 2 for the different temperature cycles. The curves obtained at 20 °C and after a heating to 150 °C show a linear and reversible behaviour. For the other temperature cycles (300, 450 and 600 °C), irreversible strains appear after the first loading cycle with the increase in temperature. This irreversible strain was weak at 300 °C, but became larger as temperature increased. The large strain results from the opening of cracks initiated by the heating. The two last loading–unloading cycles presented a more elastic behaviour with permanent strain, and the bulk modulus of elasticity is determined with these two last cycles.

The evolution of relative residual bulk modulus of elasticity for each mix as a function of temperature is presented in Fig. 8.

Contrarily to compressive strength, the modulus of elasticity is regularly damaged by the heating from 20 °C. The evolutions of modulus of elasticity are comparable for the SCC and the vibrated concrete, although the decrease is more pronounced for the vibrated concrete between 20 and 150 °C. The decrease is almost linear up to 450 °C. Beyond 450 °C, the stiffness of all specimens is very weak.

Two parts can be observed on the curves on Fig. 8. The first one is between 20 and 300 °C and corresponds to a regular decrease in modulus of elasticity. All the SCC show a modulus of elasticity higher than 50% of the initial modulus of elasticity. The modulus of elasticity of vibrated concrete is slightly lower. This decrease can be explained by the appearance of cracks (microcracking) in the specimens.

The second part of the curves, beyond 300 °C, corresponds to a very small modulus of elasticity (90% at 450 °C). It has to be noted that after a heating up to 450 and 600 °C, samples are very friable, and a lot of cracks are observed. The modulus of elasticity measured after these two

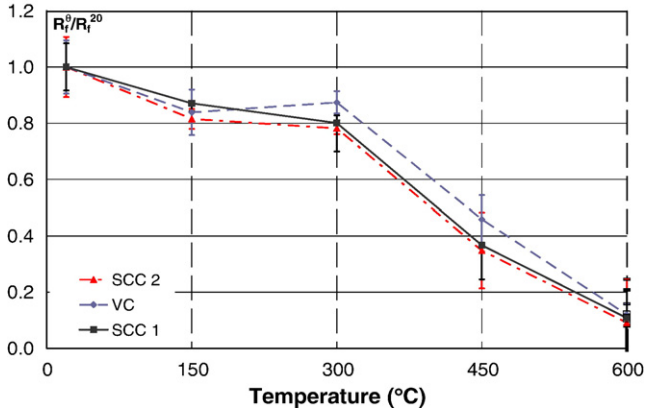

Fig. 6. Relative residual flexural strength as a function of the temperature.

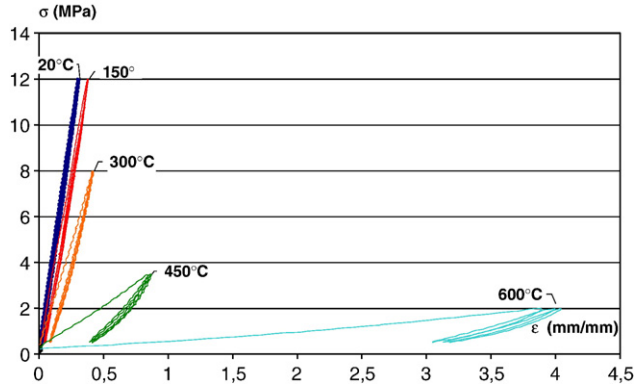

Fig. 7. Stress–strain for SCC 2.

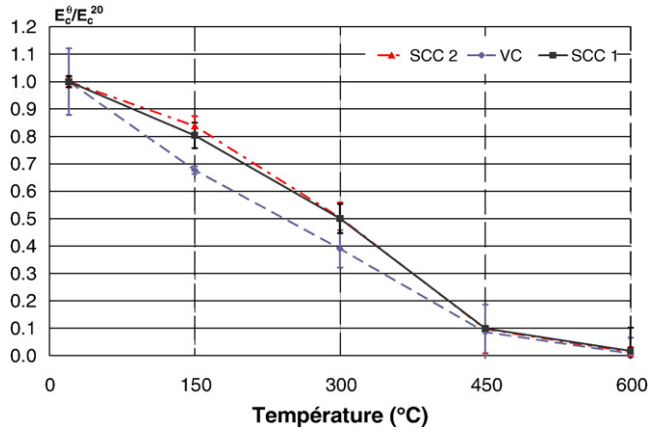

Fig. 8. Relative residual bulk modulus of elasticity as a function of temperature.

temperature cycles are therefore very spread. Phan [27] noted a loss of modulus of elasticity around 70% beyond 300 °C for several concretes having W/C ratios comprised between 0.22 and 0.57, and Kanema [20] found a decrease larger than 95% for HPC and 85% for ordinary concretes beyond 300 °C. At 600 °C, the modulus of elasticity is very low: the values vary between 0.4 and 0.6 GPa. The standard deviation after a heating up to 450 °C and 600 °C, are around 9% at 450 °C and around 1.7% at 600 °C respectively. So, with the dispersion, concretes no longer possess stiffness and therefore, modulus of elasticity can be considered negligible.

For Tolentino [36], the decrease in modulus of elasticity is due to the increase in porous volume of concrete and also to the cracking of the interfacial transition zone.

Whatever the temperature, the modulus of elasticity of vibrated concrete remains smaller than that of SCC. As the dispersion of results is generally larger than the differences between the results, we do not generalize the conclusions to all the SCC and vibrated concretes.

4.4. Concrete mass loss

Fig. 9 presents the evolutions of mass loss obtained on cylindrical specimens Ø 16×32 cm after heating. We observe that the evolution of mass loss versus temperature is very close for the three studied concretes. Between the ambient temperature and 150 °C, the variation of mass is rather weak. The loss of mass in this domain corresponds to the departure of free water contained in the capillary pores. Between 150 and 300 °C, an important increase in mass loss corresponding to 6.5% of the initial mass can be observed for all concretes.

The mass of water contained in the tested concretes comprised between 8.7 and 9.6% of the total mass. We observed that about 70% of all the water contained in the concretes has been evaporated at 300 °C. According to Kanema [20], the mass loss between 150 and 300 °C corresponds to the evaporation of bound water. At 300 °C, a mass loss corresponding to 65% to 80% of the water contained in concrete was observed for vibrated concretes. Our results are in line with these published data.

The initial water contents in the different mixes were almost the same: 199, 200 and 202 kg m^{-3}. So, as the heating rate was very low (1 °C/min), and despite the fact that the concrete porosities and permeabilities were different, water (free water and bound water) had time to escape from the concretes whatever their composition. The mass loss for the three concretes is therefore very similar.

4.5. Porosity–density

4.5.1. Porosity

Fig. 10 presents the total porosity for each mix as a function of the temperature of heating. We observed, for all the mixes, a monotonous and rather uniform increase in porosity with the temperature. Between 300 and 450 °C, the porosity increased strongly for the SCC 2 (an increase of 4% in average) while the increase was much moderated for the two other concretes (about 1%). For the values beyond 450 °C, the standard deviations are important because the specimens are very weak and friable.

Kalifa et al. [37] and Noumowé [38] attributed the increase in porosity with temperature to the departure of bound water and to the microcracking generated by differential expansion between the paste and aggregates. Noumowé et al. [39] showed by mercury intrusion porosimetry an increase in the pores sizes beyond 120 °C. Gallé et al. [40] attributed the evolution of porosity to the generation of large capillary pores. Their appearance is due to the release of adsorbed water of capillary pores and release of bound water in cement paste hydrates. Gallé et al. observe macropores correlated to microcracks observed at the surface of specimens heated beyond 250 °C. We observed from 300 °C several cracks on our specimens due to the heating, which could be correlated to the evolution of porosity and microstructure changes. Ye et al. [41] attribute the increase in porosity to the decomposition of C–S–H and CH (main hydration products). These transformations create an additional void space in the heated concretes.

Using microscopic observations, Liu et al. [21,22] compared SCC with HPC and observed changes on the microstructure with the heating. Up to 500 °C, the main physicochemical changes are the loss of water and decomposition of calcium hydroxide. These transformations lead to collapse the gel structure and create additional porosity by the alteration of the porous media (×1.5 increase in porosity between 400 and 500 °C).

If we compare the evolution of compressive strength with that of porosity, we observe both an increase in strength (≈30%) and an increase in porosity (≈10%) for the two SCC's between 150 and

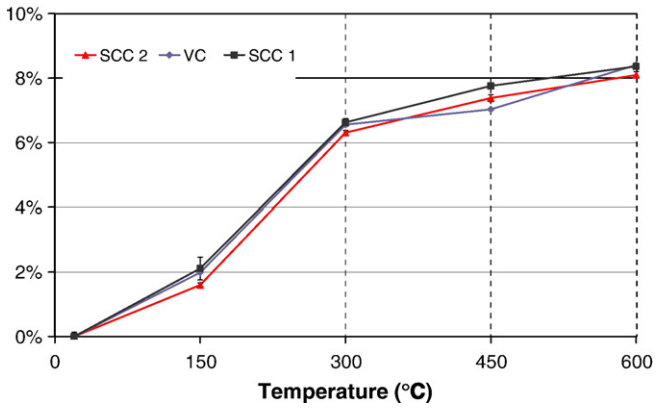

Fig. 9. Concrete mass loss as function of temperature.

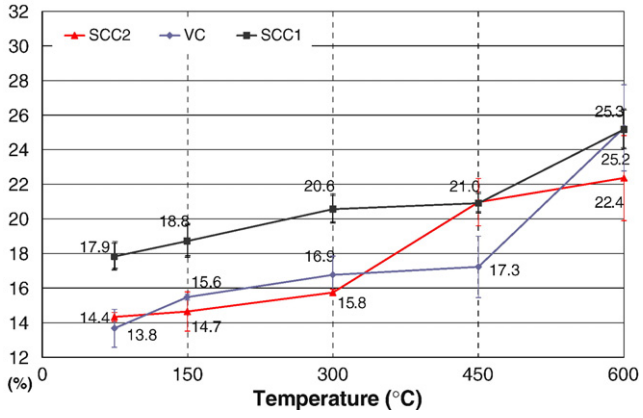

Fig. 10. Water porosity as a function of temperature.

300 °C. The increase in strength can therefore not be attributed to a decrease in porosity but rather to a modification of the bonding properties of the hydrates of cement paste. Our experimental results are therefore in line with Khoury's hypothesis concerning the creation of shorter and stronger siloxane elements Si–O–Si (with probably larger surface energies) by the loss of a part of the bonds with water in silanol groups [29]. A deeper study of the evolution of the concrete microstructure with temperature is in progress in order to better explain the strength increase.

4.5.2. Density

As for the total porosity, the evolution of apparent density (Fig. 11) depended on the composition of the concrete. Considering all the concretes (self-compacting and vibrated), we noted a decrease in density between 75 and 600 °C. For SCC 1, the overall decrease was around 5% while for the other concretes with higher strength, the density decrease was around 10%.

The decrease in apparent density with temperature between 105 °C and 400 °C has already been shown by Kalifa et al. [42] and Gaweska [43].

The decrease in density is due to the departure of water during heating (dehydration of hydrates like the C–S–H and portlandite CH). According to Bažant et al. [44], the decrease in density is associated to the thermal expansion of concrete. The evolution of density is correlated to the evolution of porosity because all these phenomena are linked.

4.6. Permeability

Fig. 12 presents the evolution of residual intrinsic permeability as a function of temperature. We noted that whatever the mix, the permeability increased monotonically between 20 and 600 °C. The increase can be considered as exponential (scale is logarithmic). For a heating up to 600 °C, the permeability is very high (permeability $>10^{-14}$ m^2). The specimens showed a dense network of open cracks. Thus, the values obtained at 600 °C can include a large error.

Between 20 and 150 °C, the permeability increased with an average factor of 10 for the 3 tested concretes. Between 150 and 300 °C, the variation was more complex. The permeability increased with a factor of 1.5 for SCC 2 and VC and 15 for SCC 1.

Beyond 300 °C, we noticed a high increase in permeability (factor comprised between 50 and 120) compared to 20 and 150 °C. Thus, the permeability evolution showed similarities with that of compressive strength. In fact, the variation between 20 and 300 °C was low comparatively to that of the domain comprised between 300 and 600 °C. Moreover, an upgrading or a small variation of the compressive strength was often observed between 150 and 300 °C. There might be a positive modification of the microstructure at these temperatures. A microstructural investigation is nevertheless necessary to strengthen this hypothesis.

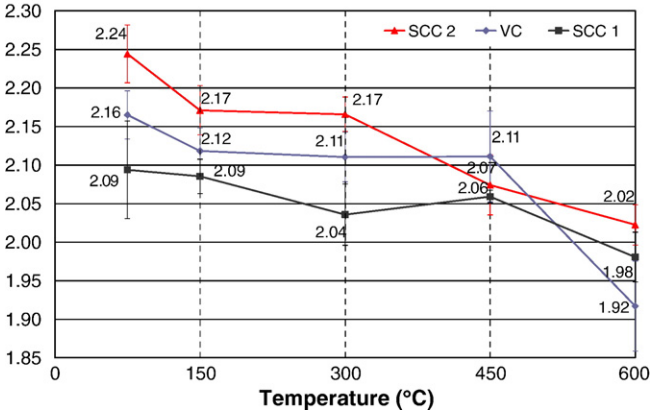

Fig. 11. Concrete density as a function of temperature.

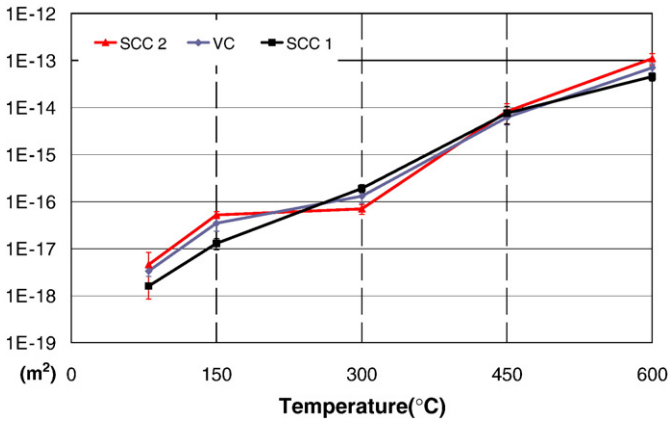

Fig. 12. Residual intrinsic permeability as a function of temperature.

According to Tsimbrovska [45], the evolution of permeability is due to the creation of pores that modify the connectivity of the porous network with the expansion of the capillary pores between 75 and 300 °C. According to Gallé et al. [40], the modification is attributed to water removal from the porous network, to adsorbed water release and to the dehydration of cement hydrates. These phenomena contribute to the increase in capillary pores sizes and to the generation of fine cracks. For temperatures higher than 300 °C, the evolution of permeability might be due not to a modification of the capillary porosity but to the deterioration of the paste leading to a modification of the fine porosity in concrete [45] or the appearance of microcracks [21,40].

So, the connectivity of the pores and microcracks are the major factors which determine the gas permeability of concrete subjected to high temperature. The connectivity of the pores acts as a dominant factor up to 300 °C. Beyond 300 °C, micro cracks become the major factor influencing the permeability [21,22,41,45].

Fig. 13 presents a comparison between our experimental results and two theoretical model results:

- Kanema's model [20] which is based on the rate of decrease in compressive strength with the temperature γ (this empirical model has been established from experimental results obtained with vibrated ordinary and high performance concretes)

$$\frac{k_v}{k_{v80}} = exp(a \cdot \gamma + b). \quad (4)$$

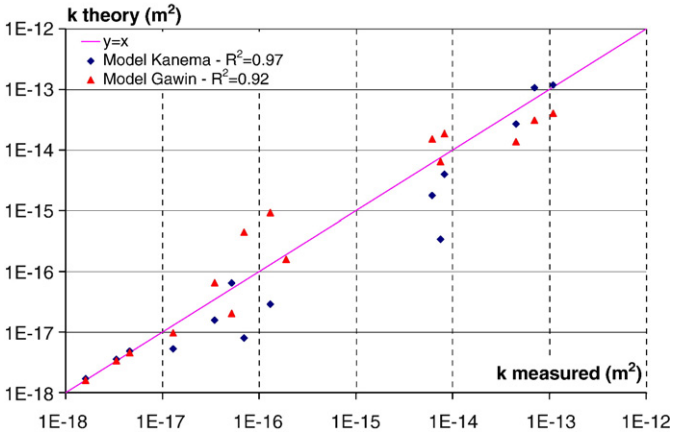

Fig. 13. Theoretical intrinsic permeability as a function of measured residual intrinsic permeability.

The values used for a and b in Eq. (4) are the same as those determined by Kanema [20]: $a = 12.012$ and $b = 0.0591$

$$\gamma = \frac{f_{c20} - f_{c(T)}}{f_{c20}}. \quad (5)$$

- Gawin et al. [46] model connects the permeability to the damage of concrete

$$k = k_0 \cdot 10^{\alpha \cdot D} \quad (6)$$

α : coefficient taking into account different kind of concrete and/or different rate of heating, here, $\alpha = 4$ (determined with our results).

D: total damage where:

$$D = 1 - \frac{E_{(T)}}{E_{20°C}}. \quad (7)$$

Fig. 13 shows a good correlation between intrinsic permeability and residual compressive strength. The correlation is also important between permeability and the damage of specimens (characterized by the evolution of modulus of elasticity). According to Liu et al. [21], the connectivity of pores and microcracking are the major factors which determine the gas permeability at high temperature. With the Eqs. (4) and (6), we showed that gas permeability is a function of compressive strength and a function of modulus of elasticity. We know that microcracking influences the evolution of compressive strength and modulus of elasticity. So, the results confirm that microcracking has an influence on the intrinsic permeability.

5. Conclusions

This study concerns the behaviour of SCC at high temperature. The residual mechanical and physical properties of two SCC and one vibrated concrete were determined after different heating cycles up to 150, 300, 450 and 600 °C.

The initial mechanical properties of the tested concretes were very close to that of the concretes used for the French National project about SCC.

During a heating at 1 °C/min, six SCC specimens spalled at about 315 °C whereas no VC specimen did spall. The risk of spalling was more pronounced for SCC than for VC.

The mechanical properties of the tested concretes (compressive and flexural strength and modulus of elasticity) generally decreased with the temperature.

Between 20 and 150 °C, a small loss of strength was observed. It was associated to an evaporation of free water as well as to an increase in porosity of the tested concretes. This porosity increase is an expansion of the pores diameters and therefore leads to an increase in permeability.

Between 150 and 300 °C, an increase in compressive strength for the SCC was observed. Nevertheless, the other mechanical properties (flexural strength and modulus of elasticity) continued to decrease in a similar way to the observed evolutions between 20 and 150 °C, due to the departure of bound water, corresponding to a large mass loss. The increase in strength could be attributed to a modification of the bonding properties of the cement paste hydrates (rehydration of the paste due to the migration of water in the pores).

Beyond 300 °C, the mechanical and physical properties of the tested concretes decreased quickly. The specimens subjected to a heating up to 600 °C showed very weak mechanical properties. The decrease of the mechanical properties was associated to that of physical properties (appearance of microcracking). Irreversible strain was observed in the heated specimens.

An increase in porosity and permeability of the tested concretes was measured. The physical property changes were due to the alteration of the porous network (departure of bound water and decomposition of hydrates) and to the microcracking. The connectivity of the pores and microcracks increased, thus the concrete permeability increased.

Models help to establish a relation between permeability and residual compressive strength and a link between permeability and concrete damage.

References

[1] H. Vanwalleghem, H. Blontrock, L. Taerwe, Spalling tests on self-compacting concrete, International RILEM Symposium on Self-Compacting Concrete, Proceedings PRO, vol. 33, 2003, pp. 855–869.
[2] E. Annerel, L. Taerwe, P. Vandevelde, Assessment of temperature increase and residual strength of SCC after fire exposure, 5th International RILEM Symposium on SCC, 2007, pp. 715–720.
[3] B. Persson, Fire resistance of SCC, Materials and Structures 37 (2004) 575–584.
[4] CERIB, Caractérisation du comportement au feu des Bétons Autoplaçants, Report DT/DCO/2001/29, 2001.
[5] L. Boström, Self-compacting concrete exposed to fire, International RILEM Symposium on Self-Compacting Concrete, Proceedings PRO, vol. 33, 2003, pp. 863–869.
[6] Étude Feu-Béton, CERIB, ATILH et organisations professionnelles de la construction française (FIB, FFB, FNTP, SNBPE, SYNAD, UNPG), réalisée au CERIB, Rapport final du projet de recherche sur le comportement au feu des bétons, 2006.
[7] NF P 18-508, AFNOR, Additions pour bétons hydrauliques — Additions calcaires — Spécifications et critères de conformité, Indice de classement : P18-508, Juillet 1995.
[8] NF EN 206-1, AFNOR, Béton — Partie 1 : Spécification, performances, production et conformité, Indice de classement : P18-325-1, Avril 2004.
[9] PNB@P, Présentation du projet National de R&D B@P, CD du colloque, Paris, 21–22 novembre 2006.
[10] AFGC, Bétons Autoplaçants — Recommandations Provisoires, Association Française Génie-Civil, 2000, 63 pp.
[11] FFB, Recommandations de mise en œuvre des BAP et BAN, Fédération Française de Génie-Civil, vol. B 62, 2003, 152 pp.
[12] Rilem Technical Committees 129-MHT, Test methods for mechanical properties of concrete at high temperatures, part 1: introduction, part 2: stress–strain relation, part 3: compressive strength for service and accident conditions, Materials and Structures 28 (181) (1995) 410–414.
[13] NF EN 12390-3, AFNOR, Essai pour béton durci — Partie 3 : Résistance à la compression des éprouvettes, Indice de classement : P18-455, Février 2003.
[14] J.M. Torrenti, P. Dantec, C. Boulay, J.F. Semblat, Projet de processus d'essai pour la détermination du module de déformation longitudinale du béton, Notes techniques, Bulletin des laboratoires des Ponts et Chaussées 4263 (1999) 79–81 n° 220 NT.
[15] NF EN 12390-5, AFNOR, Essai pour béton durci — Partie 5 : Résistance à la flexion des éprouvettes, Indice de classement : P18-433, Octobre 2001.
[16] AFPC-AFREM, sur la durabilité des bétons, Méthodes recommandées pour la mesure des grandeurs associées à la durabilité des bétons, INSA-LMDC, Toulouse, déc. 1997, pp. 11–12.
[17] M. Choinska, Effets de la température, du chargement mécanique et de leurs interactions sur la perméabilité du béton de structure, Thèse de doctorat, Ecole Centrale de Nantes, 2006.
[18] J.J. Kollek, The determination of the permeability of concrete to oxygen by the CEMBUREAU method — a recommendation, Materials and Structures 22 (1989) 225–230.
[19] L.J. Klinkenberg, The permeability of porous media to liquid and gases. American Petroleum Institute, Drilling and Production Practices (1941) 200–214.
[20] M. Kanema, Influence des paramètres de formulation et microstructuraux sur le comportement à haute température des bétons, Thèse de doctorat, Université de Cergy-Pontoise, 2007.
[21] X. Liu, G. Ye, G. De Schutter, Y. Yuan, L. Taerwe, On the mechanism of polypropylene fibres in preventing fire spalling in self-compacting and high-performance cement paste, Cement and Concrete Research 38 (2008) 487–499.
[22] X. Liu, G. Ye, G. De Schutter, Y. Yuan, Modeling the microstructure change of high performance cement paste at elevated temperature, CONMOD'08, RILEM Proceedings PRO, vol. 58, 2008, pp. 439–446.
[23] RILEM Report 38, Durability of self-compacting concrete, RILEM, 2007, pp.185.
[24] L. Boström, The performance of some self-compacting concretes when exposed to fire, SP Report (23) (2002) Sweden.
[34] [25] A. Noumowé, H. Carré, A. Daoud, H. Toutanji, High-strength self-compacting concrete exposed to fire test, Journal of Materials in Civil Engineering, Vol. 18, Issue 6, pp. 754-758.
[26] Eurocode 4 — Calcul des structures mixtes acier-béton. Partie 1-2 : Règles générales, calcul du comportement au feu, NF EN 1994-1-2. AFNOR, octobre 2005.
[27] L.T. Phan, J.R. Lawson, F.L. Davis, Effects of elevated temperature exposure on heating characteristics, spalling, and residual properties of high performance concrete, Materials and Structures 34 (2001) 83–91.
[28] W.P.S. Dias, G.A. Khoury, P.J.E. Sullivan, Mechanical properties of hardened cement paste exposed to temperatures up to 700 °C, ACI Materials Journal 87 (2) (1990) 160–166.
[29] G.A. Khoury, Compressive strength of concrete at high temperature: a reassessment, Magazine of Concrete Research 44 (1992) 291–309.
[30] Y. Xu, Y.L. Wong, C.S. Poon, M. Anson, Impact of high temperature on PFA concrete, Cement and Concrete Research 31 (2001) 1065–1073.

[31] M. Saad, S.A. Abo-El-Enein, G.B. Hanna, M.F. Kotkata, Effect of temperatures on physical and mechanical properties of concrete containing silica fume, Cement and Concrete Research 26 (1996) 669–675.
[32] N.G. Zoldner, Effect of high temperatures on concretes incorporating different aggregates, Proceeding ASTM, Philadelphia, vol. 60, 1960, pp. 1087–1108.
[33] V.M. Malhotra, H.S. Wilson, K.E. Painter, Performance of gravelstone concrete incorporating silica fume at elevated temperature, Proceeding of the Third International Conference, Trondheim (Norway), vol. 2, ACI Publication, 1989, pp. 1051–1076, SP114-51.
[34] P.K. Mehta, P.J.M. Monteiro, Concrete: Structure, Properties and Materials, Prentice-Hall, Englewood Cliffs, N.J, 1993.
[35] Wei Li, Zhen-Hai Guo, Experimental research on the strength and deformation properties of concrete exposed to high temperature, Journal of Building Structures (China) 14 (1) (1993) 8–16.
[36] E. Tolentino, F.S. Lameiras, A.M. Gomes, C.A. Rigo da Silva, W.L. Vasconcelos, Effects of high temperature on residual performance of Portland cement concrete, Materials Research 5 (2002) 301–307 N°3.
[37] P. Kalifa, M. Tsimbrovska, Comportement des BHP à hautes températures — Etat de la question et résultats expérimentaux, Cahier du CSTB n°3078, 1998.
[38] N.A. Noumowé, Effet de hautes températures (20–600 °C) sur le béton. Cas particulier du Béton à hautes températures, Thèse de doctorat de l'INSA de Lyon, 1995.
[39] A.N. Noumowé, P. Clasters, G. Debicki, J.L. Costaz, Transient heating effect on high strength concrete, Nuclear Engineering and Design 166 (1) (1996) 99–108.
[40] C. Gallé, J. Sercombe, Permeability and pore structure evolution of silico-calcareous and hematite high-strength concretes submitted to high temperatures, Materials and Structures 34 (2001) 619–628.
[41] G. Ye, X. Liu, G. De Schutter, L. Taerwe, P. Vandevelde, Phase distribution and microstructural changes of SCC at elevated temperatures, Cement and Concrete Research 37 (2007) 978–987.
[42] P. Kalifa, F.D. Menneteau, D. Quenard, Spalling and pore pressure in HPC at high temperature, Cement and Concrete Research 30 (2000) 1915–1927.
[43] H.I. Gaweska, Comportement à haute température des bétons à haute performance-évolution des principales propriétés mécaniques. Thèse de doctorat, Ecole Nationale des Ponts et Chaussées et Ecole Polytechnique de Croatie, 2004.
[44] Z.P. Bazant, M.F. Kaplan, Concrete at High Temperatures: Material Properties and Mathematical Models, Pearson Education, 1996.
[45] M. Tsimbrovska, P. Kalifa, D. Quenard, High Performance Concretes at Elevated Temperatures — Permeability and Microstructure, SMIRT 14, Lyon, France, August 17–22, 1997, pp. 475–482.
[46] D. Gawin, F. Pesavento, B.A. Schlefler, Simulation of damage-permeability coupling in hygrothermo-mechanical analysis of concrete at high temperature, Communications in Numerical Methods in Engineering 18 (2002) 113–119.